Murakami, H. Tamamura, *ACS Chem, Biol.,* **8**, 2235(2013)

17) (a)A. Santini, V. Barone, A. Bavoso, E. Benedetti, B. Di Blasio, F. Fraternali, F. Lelj, V. Pavone, C. Pedone, M. Crisma, G. M. Bonora, C. Toniolo, *Int. J. Biol. Macromol.,* **10**, 292(1988); (b) Y. Demizu, Y. Yabuki, M. Doi, Y. Sato, M. Tanaka, M. Kurihara, *J. Pept. Sci.,* **18**, 466(2012)

18) (a)A. Banerjee, S. Raghothama, P. Balaram, *J. Chem. Soc., Perkin Trans. 2,* 1997, 2087; (b)Y. Demizu, N. Yamagata, Y. Sato, M. Doi, M. Tanaka, H. Okuda, M. Kurihara, *J. Pept. Sci.,* **16**, 153(2010)

19) (a)Y. Demizu, N. Yamagata, S. Nagoya, Y. Sato, M. Doi, M. Tanaka, K. Nagasawa, H. Okuda, M. Kurihara, *Tetrahedron,* **67**, 6155(2011); (b)N. Yamagata, Y. Demizu, Y. Sato, M. Doi, M. Tanaka, K. Nagasawa, H. Okuda, M. Kurihara, *Tetrahedron Lett.,* **52**, 798(2011)

20) (a)S. Juliá, J. Guixer, J. Masana, J. Rocas, S. Colonna, R. Annuziata, H. Molinari, *J. Chem. Soc., Perkin Trans. 1,* 1982, 1317; (b)S. Juliá, J. Masana, J. C. Vega, *Angew. Chem., Int. Ed. Engl.,* **19**, 929(1980)

21) (a)K. Akagawa, K. Kudo, *Adv. Synth. Catal.,* **353**, 843(2011); (b)A. Berkessel, B. Koch, C. Toniolo, M. Rainaldi, Q. B. Broxterman, B. Kaptein, *Biopolymers(Pept. Sci.),* **84**, 90 (2006); (c)D. R. Kelly, T. T. T. Bui, E. Caroff, A. F. Drake, S. M. Roberts, *Tetrahedron Lett.,* **45**, 3885(2004); (d)R. Takagi, A. Shiraki, T. Manabe, S. Kojima, K. Ohkata, *Chem. Lett.,* 2000, 366

22) M. Nagano, M. Doi, M. Kurihara, H. Suemune, M. Tanaka, *Org. Lett.,* **12**, 3564(2010)

23) G. Carrea, S. Colonna, D. R. Kelly, A. Lazcano, G. Ottolina, S. M. Roberts, *Trends Biotechnol.,* **23**, 507(2005)

24) (a)L. A. Zella, C.-Y. Chang, D. P. McDonnell, J. W. Pike, *Arch. Biochem. Biophys.,* **460**, 206(2007); (b)J. W. Pike, P. Pathrose, O. Barmina, C.-Y. Chang, D. P. McDonnell, H. Yamamoto, N. K. Shevde, *J. Cell. Biochem.,* **88**, 252(2003); (c)P. Pathrose, O. Barmina, C.-Y. Chang, D. P. McDonnell, N. K. Shevde, J. W. Pike, *J. Bone Miner. Res.,* **17**, 2196(2002)

25) (a)Y. Mita, K. Dodo, K. Noguchi-Yachide, Y, Hashimoto, M. Ishikawa, *Bioorg. Med. Chem.,* **21**, 993(2013); (b)P. Nandhikonda, W. Z. Lynt, M. M. McCallum, T. Ara, A. M. Baranowski, N. Y. Yuan, D. Pearson, D. D. Bikle, R. K. Guy, L. A. Arnold, *J. Med. Chem.,* **55**, 4640(2012)

26) Y. Demizu, S. Nagoya, M. Shirakawa, M. Kawamura, N. Yamagata, Y. Sato, M. Doi, M. Kurihara, *Bioorg. Med. Chem. Lett.,* **23**, 4292(2013)

27) Unpublished results.

28) Y. Demizu, T. Takahashi, F. Kaneko, Y. Sato, H. Okuda, E. Ochiai, K. Horie, K. Takagi, S. Kakuda, M. Takimoto-Kamimura, M. Kurihara, *Bioorg. Med. Chem. Lett.,* **21**, 6104 (2011)

29) (a)I. Nakase, H. Akita, K. Kogure, A. Gráslund, Ü. Langel, H. Harashima, S. Futaki, *Acc. Chem. Res.,* **45**, 1132(2012); (b)J. M. Hyman, E. I. Geihe, B. M. Trantow, B. Parvin, P. A. Wender, *Proc. Natl. Acad. Sci. U.S.A.,* **109**, 13225(2012); (c)G. K. Seward, Q. Wei, I. J. Dmochowski, *Bioconjugate Chem.,* **19**, 2129(2008); (d)B. Gupta, T. S. Levchenko, V. P. Torchilin, *Adv. Drug Deliv. Rev.,* **57**, 637(2005); (e)J. Oehlke, P. Birth, E. Klauschenz, B. Wiesner, M. Beyermann, A. Oksche, M. Bienert, *Eur. J. Biochem.,* **269**, 4025(2002)

30) (a)T. B. Potocky, A. K. Menon, S. H. Gellman, *J. Am. Chem. Soc.,* **127**, 3686(2005); (b)S. Wada, Y. Hashimoto, Y. Kawai, K. Miyata, H. Tsuda, O. Nakagawa, H. Urata, *Bioorg. Med. Chem.,* **21**, 7669(2013)

31) H. Yamashita, Y. Demizu, T. Shoda, Y. Sato, M. Oba, M. Tanaka, M. Kurihara, *Bioorg. Med. Chem.,* **22**, 2403(2014)

PROFILE

出水庸介　国立医薬品食品衛生研究所有機化学部・室長　博士（薬学）
〔経歴〕2004 年徳島文理大学香川薬学部助手。2006 年九州大学大学院薬学府博士後期課程修了。2006 年長崎大学大学院医歯薬学総合研究科助教。2008 年国立医薬品食品衛生研究所有機化学部研究員，2011 年同主任研究官を経て 2011 年 12 月より現職。この間，2012-13 年ウィスコンシン大学（S. H. Gellman 教授）JSPS 海外特別研究員。〔専門〕有機合成化学，創薬化学，ペプチド化学。〔連絡先〕e-mail: demizu@nihs.go.jp

三澤隆史　国立医薬品食品衛生研究所有機化学部・研究員　博士（薬学）
〔経歴〕2011 年日本学術振興会特別研究員（DC2），2012 年東京大学大学院薬学系研究科博士後期課程修了。2012 年ウィスコンシン大学化学科博士研究員。2013 年東京大学分子細胞生物学研究所助教。2014 年より現職。〔専門〕医薬化学，ペプチド化学。〔連絡先〕e-mail: misawa@nihs.go.jp

栗原正明　国立医薬品食品衛生研究所有機化学・部長　薬学博士
〔経歴〕1987 年東京大学大学院薬学研究科博士課程修了。1987 年国立医薬品食品衛生研究所有機化学部研究官，1992 年同主任研究官，1995 年同第一室長，2001 年同第二室長，2011 年より現職。2012 年東京工業大学大学院連携教授併任（生体分子機能工学専攻）。1991-92 年ケンタッキー大学博士研究員。〔専門〕有機合成化学，創薬化学，計算機化学。〔連絡先〕e-mail: masaaki@nihs.go.jp

Identification of a Wide Range of Motifs Inhibitory to Shiga Toxin by Affinity-Driven Screening of Customized Divalent Peptides Synthesized on a Membrane

Mihoko Kato, Miho Watanabe-Takahashi, Eiko Shimizu, Kiyotaka Nishikawa

Faculty of Life and Medical Sciences, Doshisha University, Kyoto, Japan

Shiga toxin (Stx), a major virulence factor of enterohemorrhagic *Escherichia coli*, binds to target cells through a multivalent interaction between its B-subunit pentamer and the cell surface receptor globotriaosylceramide, resulting in a remarkable increase in its binding affinity. This phenomenon is referred to as the "clustering effect." Previously, we developed a multivalent peptide library that can exert the clustering effect and identified Stx neutralizers with tetravalent peptides by screening this library for high-affinity binding to the specific receptor-binding site of the B subunit. However, this technique yielded only a limited number of binding motifs, with some redundancy in amino acid selectivity. In this study, we established a novel technique to synthesize up to 384 divalent peptides whose structures were customized to exert the clustering effect on the B subunit on a single cellulose membrane. By targeting Stx1a, a major Stx subtype, the customized divalent peptides were screened to identify high-affinity binding motifs. The sequences of the peptides were designed based on information obtained from the multivalent peptide library technique. A total of 64 candidate motifs were successfully identified, and 11 of these were selected to synthesize tetravalent forms of the peptides. All of the synthesized tetravalent peptides bound to the B subunit with high affinities and effectively inhibited the cytotoxicity of Stx1a in Vero cells. Thus, the combination of the two techniques results in greatly improved efficiency in identifying biologically active neutralizers of Stx.

Infection with enterohemorrhagic *Escherichia coli* (EHEC) causes bloody diarrhea and hemorrhagic colitis, sometimes followed by fatal systemic complications, such as acute encephalopathy and hemolytic-uremic syndrome (HUS) (1–6). In 2011, unprecedented outbreaks of *E. coli* O104:H4 occurred in the European Union (EU), particularly in Germany, with more than 4,000 cases of infection and 50 fatalities (7, 8). Since antibiotic use is controversial (9–11), novel therapeutic strategies against the infection are urgently required. EHEC produces Shiga toxin (Stx) as a major virulence factor; therefore, one of the most promising approaches is to develop an Stx neutralizer that effectively binds to and inhibits Stx.

Stx, a typical ribotoxin, is present in various forms that can be classified into two subgroups, Stx1 and Stx2, each of which has various closely related subtypes: Stx1a, -1c, and -1d and Stx2a, -2b, -2c, -2d, -2e, -2f, and -2g, respectively (12–14). Each Stx subtype consists of a catalytic A subunit and a B-subunit pentamer, which is responsible for high-affinity binding to the functional cell surface receptor Gb3 [Galα(1-4)-Galβ(1-4)-Glcβ-ceramide] (4, 15, 16), or Gb4 [GalNAcβ(1-3)-Galα(1-4)-Galβ(1-4)-Glcβ-ceramide], which is preferred by Stx2e (17). Each B subunit has three distinctive binding sites (sites 1, 2, and 3) for the trisaccharide moiety of Gb3 (18, 19), resulting in the formation of a multivalent interaction between the B-subunit pentamer and Gb3. This type of interaction is known to markedly increase the binding affinity a millionfold and is generally known as the "clustering effect."

Previously, we developed a multivalent peptide library that can exert the clustering effect and identified Stx neutralizers with tetravalent peptides by screening this library based on high-affinity binding to specific receptor-binding sites (20–22). By targeting one of the receptor-binding sites (site 3) of subtype Stx2a which is most closely associated with high disease severity (23, 24), we identified four tetravalent peptides that bind to Stx2a with high

affinity and specificity as novel peptide-based neutralizers (20). One of the neutralizers, PPP-tet, protected mice from a fatal dose of *E. coli* O157:H7 (20) and inhibited the lethal effect of intravenously administered Stx2a in a nonhuman primate model (25). Recently, by targeting receptor-binding site 1 of Stx1a, the most frequently observed subtype, we identified tetravalent peptide MMA-tet (22). Interestingly, MMA-tet strongly inhibited Stx1a and Stx2a with greater potency than that of PPP-tet as well as rescuing mice from the lethality caused by the infection by *E. coli* O157:H7, which produces both toxins. This multivalent peptide library technique, however, can yield only a limited number of binding motifs for the intended receptor-binding region of the B subunit, with redundancy of amino acid selectivity at some positions.

In this study, we established a novel technique to determine a wide range of binding motifs for the B subunit by directly screening hundreds of divalent peptides on a membrane whose struc-

tures were customized to exert the clustering effect. By targeting one of the receptor-binding sites (site 2) of the Stx1a B subunit, a site which plays a significant role in the receptor binding of Stx1a (18, 26), we successfully identified 11 peptide-based neutralizers of Stx1a using this novel technology combined with multivalent peptide library screening. Screening the multivalent peptide library alone could not identify a biologically active inhibitor of this site. Thus, the combination of the two techniques will provide a powerful strategy to develop customized neutralizers for a restricted area of the receptor-binding region of the B subunit, enabling the identification of tailored neutralizers for each Stx subtype with highly conserved structural similarity.

MATERIALS AND METHODS

Materials. Recombinant Stx1a, histidine-tagged Stx1a B subunit (1BH), and 1BH with a single-amino-acid substitution (1BH-G62A) were prepared as described previously (27). The amino-PEG$_{500}$-UC540 membrane (Intavis Bioanalytical Instruments AG, Germany) used for the spot synthesis of peptides was purchased from PerkinElmer, Tokyo, Japan. Porcine erythrocyte Gb3 and egg phosphatidylcholine (PC) were purchased from Wako Pure Industries, Osaka, Japan.

Peptides and peptide library screening. Tetravalent peptides and tetravalent peptide libraries were synthesized using N-α-9-fluorenylmethoxy carbonyl (FMOC)-protected amino acids and standard BOP [benzotriazol-1-yloxytris(dimetylamino)phosphonium hexafluorophosphate]/HOB (1-hydroxybenzotriazole hydrate) coupling chemistry as described previously (20). A Met-Ala sequence was included at the amino terminus of each library peptide to verify the identity and origin of the peptides being sequenced and to qualify the peptides. Recombinant 1BH or 1BH-G62A (0.5 mg protein) bound to Ni^{2+} beads was incubated with 300 μg of a given library peptide in phosphate-buffered saline (PBS) overnight at 4°C. After extensive washing, the bound peptides were sequenced on an Applied Biosystems model 477A protein sequencer. To calculate the relative amino acid preference at each degenerate position, the corrected quantities of amino acids in the peptides recovered from the 1BH beads were compared with those recovered from the 1BH-G62A beads to calculate the abundance ratios of amino acids (20).

ELISA of the binding between 1BH and inhibitory peptides. The indicated amounts of the tetravalent peptide dissolved in PBS were applied as a coating onto each well of a 96-well enzyme-linked immunosorbent assay (ELISA) plate and incubated for 24 h at 4°C. After blocking, the plate was incubated with 1BH or 1BH-G62A (1 μg/ml) for 1 h at room temperature. Bound 1BH was detected using rabbit anti-Stx1a antiserum as described previously (20).

Cytotoxicity assay. Subconfluent Vero cells were cultured in a 96-well plate in Dulbecco's modified Eagle's medium (DMEM) supplemented with 10% fetal calf serum and treated with Stx1a (1 pg/ml) in the absence or presence of a given tetravalent peptide for 72 h at 37°C. The relative number of living cells was determined using cell counting kit 8 (Dojindo, Kumamoto, Japan) as described previously (22).

Spot synthesis of peptides on cellulose membrane. Basic spot synthesis of peptides on a cellulose membrane was performed as described previously (28, 29) using the ResPep SL spot synthesizer (Intavis Bioanalytical Instruments AG, Cologne, Germany). The density of peptides synthesized on a membrane was controlled by using a mixture of FMOC-βAla-OH and Boc-βAla-OH (Watanabe Chemical Industries, Japan) at different ratios (100:0, 30:70, or 10:90, respectively) for the first cycle. *t*-Butyloxycarbonyl (Boc) is resistant to the deprotection procedure and inhibits the subsequent elongation reaction. The spacer length of the peptide was controlled by the number of amino hexanoic acids following the first βAla. After the addition of amino hexanoic acid(s), FMOC-Lys(F-MOC)-OH (Watanabe Chemical Industries) was used for the next cycle to bifurcate the peptide chain for subsequent motif synthesis. This step was omitted for monovalent peptide synthesis. The successful synthesis of each peptide was confirmed by staining the membrane using bromophe-

nol blue (1% in N,N'-dimethylformamide), which reacts to free amino residues. Free amino residues are produced only after the completion of all the reactions and before the deprotection of the side chain residues. After destaining with N,N'-dimethylformamide, the membrane was used in the binding assay. As a positive control for Stx B-subunit binding, Gb3 (0.1 μg) mixed with PC (1 μg) was directly spotted on the membrane.

Binding assay of 1BH or 1BH-G62A to divalent peptides synthesized on the membrane. After blocking with 5% skim milk in PBS, the membrane (prepared as described above) was blotted with the indicated concentration of ^{125}I-1BH or ^{125}I-1BH-G62A (1 × 10^6 to 2 × 10^6 cpm/μg protein) for 1 h at room temperature. After extensive washing, the radioactivity bound to each peptide spot was quantitated as a pixel value using a BAS 2500 bioimaging analyzer system (GE Healthcare, Amersham, United Kingdom). In another detection system, the membrane was blotted with 1.0 μg/ml 1BH for 1 h at room temperature. After extensive washing, bound 1BH was detected using rabbit anti-Stx1a antiserum as described previously (22) and quantitated as a pixel value using Image-Quant LAS 500 (GE Healthcare).

Kinetic analysis of the binding between inhibitory peptides and immobilized 1BH. The binding of tetravalent peptides to immobilized 1BH was quantified using a Biacore T100 system instrument (GE Healthcare Sciences, USA) as described previously (20). The resonance unit is an arbitrary unit (AU) used by the Biacore system. Binding kinetics were analyzed using Biaevaluation software, v1.1.1 (GE Healthcare).

RESULTS

Tetravalent peptide library screening identified a peptide motif that specifically binds 1BH through site 2. A tetravalent peptide library is comprised of peptides containing a polylysine core that bifurcates at both ends with four randomized peptides (20). The library was screened for the ability to bind to wild-type 1BH but not to 1BH-G62A, which contains a mutation in one of the receptor-binding sites (site 2). Site 2 has been shown to play an essential role in the receptor binding of Stx1a (26). A tetravalent peptide library with a fixed Arg at position 4 (the XRX library) was used for the first round of selection, based on the previous observation that Stx1a prefers clustered Args in its binding motifs (22). As shown in Fig. 1A, Arg was strongly selected at positions 1, 5, and 7, and His was selected at position 5. Based on this result, a second tetravalent peptide library with clustered Args (the XRR library) was screened to further refine peptide selection. Lys was strongly selected at position 1, and both Arg and His were selected at position 3. Based on these results, we identified KRRRRRR as a candidate motif. A tetravalent form of this peptide with the same core structure was synthesized and referred to as KRR-tet. As shown in Fig. 1B, KRR-tet bound efficiently to 1BH, whereas the binding to 1BH-G62A was less efficient. Under the same conditions, MA-tet, which has the same core structure but lacks the binding motif, did not bind to either of the B subunits (data not shown). These results indicate that KRR-tet specifically binds to the B subunit through site 2. KRR-tet, however, was found to be cytotoxic due to its highly basic nature (Fig. 1C) and thus did not inhibit the cytotoxicity of Stx1a in Vero cells, in contrast to MMA-tet (Fig. 1D).

Establishment of a technique to synthesize peptides on a membrane that can exert the clustering effect on the Stx1a B subunit. KRR-tet has an Arg cluster at positions 4 to 7; this cluster is also observed in MMA-tet, indicating that the motif is commonly required for the efficient binding to the Stx1a B subunit. Based on this motif, we tried to identify a series of site 2-targeted binding motifs by establishing a novel technique in which hun-

A

1st-libarary	position						
	1	2	3	4	5	6	7
(MA-XXXRXXX-AU)$_4$-3Lys				R			
; XRX-library	R (1.31)	R (1.23)	R (1.28)		R (1.31)	R (1.22)	R (1.32)
	M (1.15)	H (1.11)	H (1.1)		H (1.21)		H (1.1)

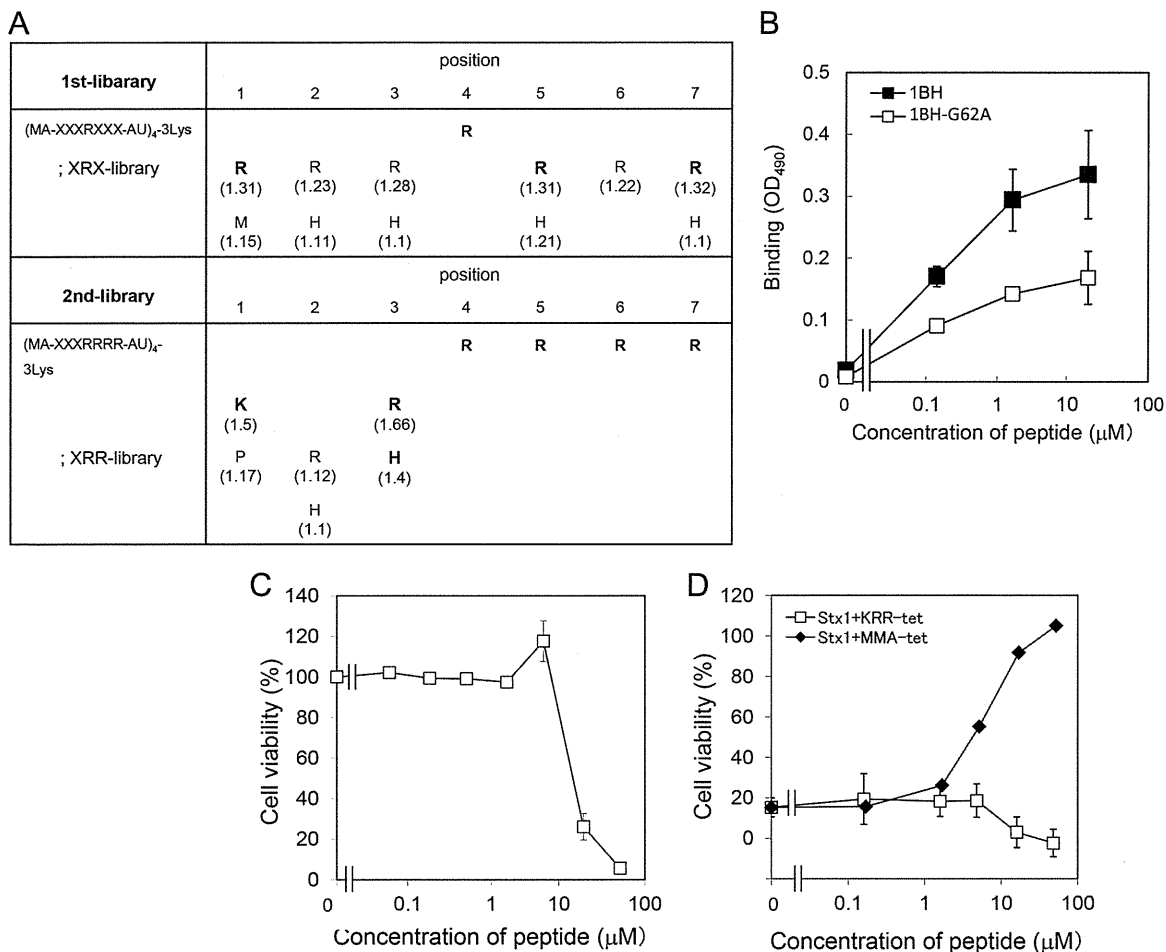| 2nd-library	position						
	1	2	3	4	5	6	7
(MA-XXXRRRR-AU)$_4$-3Lys				R	R	R	R
; XRR-library	K (1.5)		R (1.66)				
	P (1.17)	R (1.12)	H (1.4)				
		H (1.1)					

B

C

D

FIG 1 Identification of a peptide motif that specifically binds to Stx1a B subunit through site 2 by using tetravalent peptide library screening. (A) The tetravalent peptide library was comprised of tetravalent peptides with a polylysine core bifurcating at both ends with four randomized peptides. The peptide library for the first screening had the sequence Met-Ala-X-X-X-R-X-X-X-Ala-U (U, amino hexanoic acid), where X indicates all amino acids except Cys. Screening of the library was performed to identify tetravalent peptides that bound to 1BH but not to 1BH-G62A. For the second screening, a peptide library with fixed Args at positions 4 to 7 (XRR library) was used. Values in parentheses indicate relative selectivities for the amino acids. Bold letters indicate amino acids that were strongly selected. Each screening was performed twice; representative values are shown. (B) The binding of 1BH or 1BH-G62A (1 μg/ml) to KRR-tet at the indicated concentrations was examined using ELISA (mean ± standard error, $n = 3$). (C) The effect of KRR-tet on the cell viability in Vero cells was examined by the cytotoxicity assay. Data are presented as a percentage of the control value (mean ± standard error, $n = 4$). (D) The effect of KRR-tet or MMA-tet on the cytotoxic activity of Stx1a (1 pg/ml) in Vero cells was examined by the cytotoxicity assay (mean ± standard error, $n = 4$).

dreds of peptides with the Arg cluster were synthesized in a divalent form on a cellulose membrane and screened for high-affinity binding to 1BH but not to 1BH-G62A. We also optimized the structure of the peptide synthesized on the membrane (Fig. 2A). A divalent form of the peptide, KRRRRRR, was found to exert the clustering effect and exhibited markedly increased binding to 1BH compared to the monovalent form (Fig. 2B). Under the same conditions, Gb3 blotted on the membrane was specifically detected by 1BH. Using the divalent peptide, we found that a spacer of one amino hexanoic acid functioned most efficiently and that the higher density yielded higher binding efficacy (Fig. 2B). We further examined the binding of other divalent peptides. The divalent form of MMARRRR, a binding motif present in MMA-tet, also efficiently bound to 1BH in a dose-dependent manner when one amino hexanoic acid was used as a spacer (Fig. 2C). Similar density dependency was observed for the divalent peptide (Fig. 2B). The divalent form of AAARRRR, another binding motif previ-

ously determined for 1BH (22), could still efficiently bind to 1BH. In contrast, the divalent form of AAADDDD, in which all Args of AAARRRR were replaced with Asps, completely lost binding activity (Fig. 2C), confirming the requirement of the Arg cluster in the binding motif.

Screening of divalent peptides synthesized on a membrane successfully identified a wide range of peptide motifs that specifically bind to the Stx1a B subunit through site 2. Using the optimized conditions identified above, 380 divalent peptides containing the Arg cluster and shuffled amino acids at motif positions 1 to 3 were synthesized on a cellulose membrane. One group had the XXA-RRRR motif, and the other group had the AAX-RRRR motif, respectively, where X indicates a fixed amino acid as indicated (Fig. 3A). The divalent peptide with the original motif KRR-RRRR was also synthesized. The membrane was blotted with [125]I-1BH or [125]I-1BH-G62A (Fig. 3B), and the radioactivity bound to each peptide spot was quantitated and analyzed. Divalent peptides
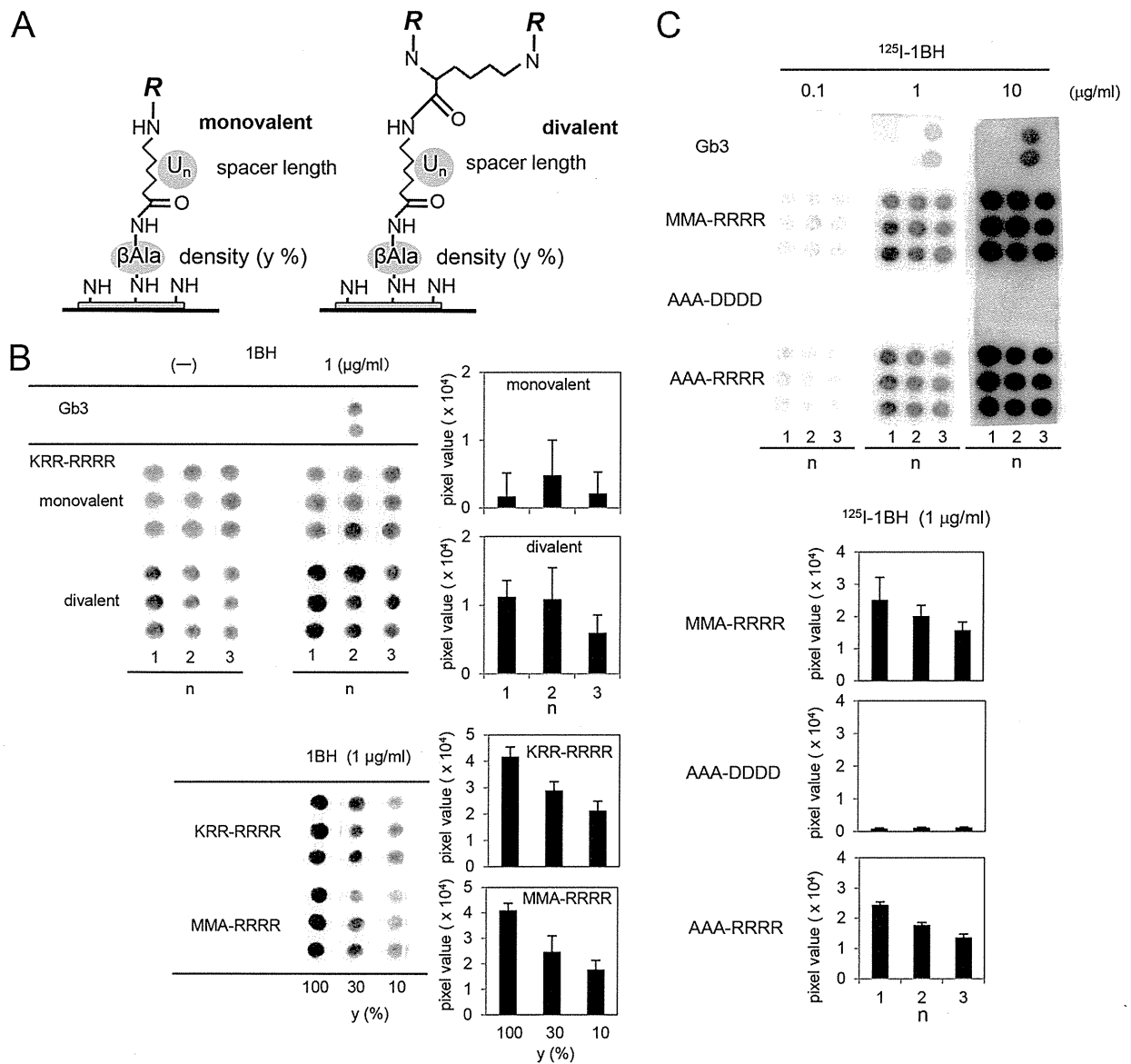
— 61 —

FIG 2 Optimization of the structure of the peptides synthesized on a membrane to exert the clustering effect. (A) The structure of a monovalent or a divalent peptide synthesized on a cellulose membrane is shown as described in Materials and Methods (density: y = 10, 30, or 100%; spacer length: n = 1, 2, or 3; U indicates amino hexanoic acid; R = Met-Ala-[indicated motif]-Ala). (B) The monovalent or the divalent form of the KKKRRRR motif was synthesized with different spacer lengths in triplicate (y = 100%, upper panel). The divalent form of the KKKRRRR or MMARRRR motif was synthesized with different densities (n = 1, lower panel). The membrane was blotted with 1.0 μg/ml of 1BH. Bound 1BH was detected using rabbit anti-Stx1a antiserum and quantitated as a pixel value. Each value is shown after subtraction of the control value obtained without 1BH. (C) Divalent peptides with the MMARRRR, AAADDDD, or AAARRRR motif were synthesized on a membrane with different spacer lengths (y = 100%). The membrane was blotted with the indicated concentration of ^{125}I-1BH, and the radioactivity bound to each peptide was detected (upper panel) and quantitated. Data obtained with 1.0 μg/ml of ^{125}I-1BH are shown (lower panel).

with a normalized value of ^{125}I-1BH binding (1BH-binding value) greater than 1.14 were selected and then resorted in descending order of the product (1BH × ratio) of the 1BH-binding value and the normalized ratio (1BH/G62A ratio), as shown in Table S1 in the supplemental material. A total of 64 peptides with 1BH × ratio values greater than 1.3 were identified as candidate motifs. These 64 divalent peptides were synthesized on a membrane (Fig. 4A) and blotted with different concentrations of ^{125}I-1BH or ^{125}I-1BH-G62A (Fig. 4B). The radioactivity bound to each peptide was quantitated and analyzed (see Fig. S1 in the supplemental mate-

rial). Among these divalent peptides, 11 motifs were selected based on the binding intensity and specificity of 1BH, excluding peptide motifs that had tandem basic amino acids in the first three amino acids (e.g., KHA or KKA). The exclusion was implemented to avoid selecting potentially cytotoxic motifs.

Tetravalent peptides with the identified motifs bind to 1BH through site 2 with high affinities. Tetravalent peptides with the 11 motifs identified above were synthesized using the same core structure as described in Materials and Methods and were referred to as NKA-tet, IIA-tet, KGA-tet, KMA-tet, KFA-tet, FRA-tet,

− 62 −

A

|	1	2	3	4	5	6	7	8	9	10	11	12	13	14	15	16	17	18	19	20	21	22	23	24
A					AAA	ARA	ANA	ADA	AQA	AEA	AGA	AHA	AIA	ALA	AKA	AMA	AFA	APA	ASA	ATA	AWA	AYA	AVA	RAA
B	RRA	RNA	RDA	RQA	REA	RGA	RHA	RIA	RLA	RKA	RMA	RFA	RPA	RSA	RTA	RWA	RYA	RVA	RAA	NRA	NNA	NDA	NQA	NEA
C	NGA	NHA	NIA	NLA	NKA	NMA	NFA	NPA	NSA	NTA	NWA	NYA	NVA	DAA	DRA	DNA	DDA	DQA	DEA	DGA	DHA	DIA	DLA	DKA
D	DMA	DFA	DPA	DSA	DTA	DWA	DYA	DVA	QAA	QRA	QNA	QDA	QQA	QEA	QGA	QHA	QIA	QLA	QKA	QMA	QFA	QPA	QSA	QTA
E	QWA	QYA	QVA	EAA	ERA	ENA	EDA	EQA	EEA	EGA	EHA	EIA	ELA	EKA	EMA	EFA	EPA	ESA	ETA	EWA	EYA	EVA	GAA	GRA
F	GNA	GDA	GQA	GEA	GGA	GHA	GIA	GLA	GKA	GMA	GFA	GPA	GSA	GTA	GWA	GYA	GVA	HAA	HRA	HNA	HDA	HQA	HEA	HGA
G	HHA	HIA	HLA	HKA	HMA	HFA	HPA	HSA	HTA	HWA	HYA	HVA	IAA	IRA	INA	IDA	IQA	IEA	IGA	IHA	IIA	ILA	IKA	IMA
H	IFA	IPA	ISA	ITA	IWA	IYA	IVA	LAA	LRA	LNA	LDA	LQA	LEA	LGA	LHA	LIA	LLA	LKA	LMA	LFA	LPA	LSA	LTA	LWA
I	LYA	LVA	KAA	KRA	KNA	KDA	KQA	KEA	KGA	KHA	KIA	KLA	KKA	KMA	KFA	KPA	KSA	KTA	KWA	KYA	KVA	MAA	MRA	MNA
J	MDA	MQA	MEA	MGA	MHA	MIA	MLA	MKA	MMA	MFA	MPA	MSA	MTA	MWA	MYA	MVA	FAA	FRA	FNA	FDA	FQA	FEA	FGA	FHA
K	FIA	FLA	FKA	FMA	FFA	FPA	FSA	FTA	FWA	FYA	FVA	PAA	PRA	PNA	PDA	PQA	PEA	PGA	PHA	PIA	PLA	PKA	PMA	PFA
L	PPA	PSA	PTA	PWA	PYA	PVA	SAA	SRA	SNA	SDA	SQA	SEA	SGA	SHA	SIA	SLA	SKA	SMA	SFA	SPA	SSA	STA	SWA	SYA
M	SVA	TAA	TRA	TNA	TDA	TQA	TEA	TGA	THA	TIA	TLA	TKA	TMA	TFA	TPA	TSA	TTA	TWA	TYA	TVA	WAA	WRA	WNA	WDA
N	WQA	WEA	WGA	WHA	WIA	WLA	WKA	WMA	WFA	WPA	WSA	WTA	WWA	WYA	WVA	YAA	YRA	YNA	YDA	YQA	YEA	YGA	YHA	YIA
O	YLA	YKA	YMA	YFA	YPA	YSA	YTA	YWA	YYA	YVA	VAA	VRA	VNA	VDA	VQA	VEA	VGA	VHA	VIA	VLA	VKA	VMA	VFA	VPA
P	VSA	VTA	VWA	VYA	VVA	AAR	AAN	AAD	AAQ	AAE	AAG	AAH	AAI	AAL	AAK	AAM	AAF	AAP	AAS	AAT	AAW	AAY	AAV	KRR

B

^{125}I -1BH

^{125}I -1BH-G62A
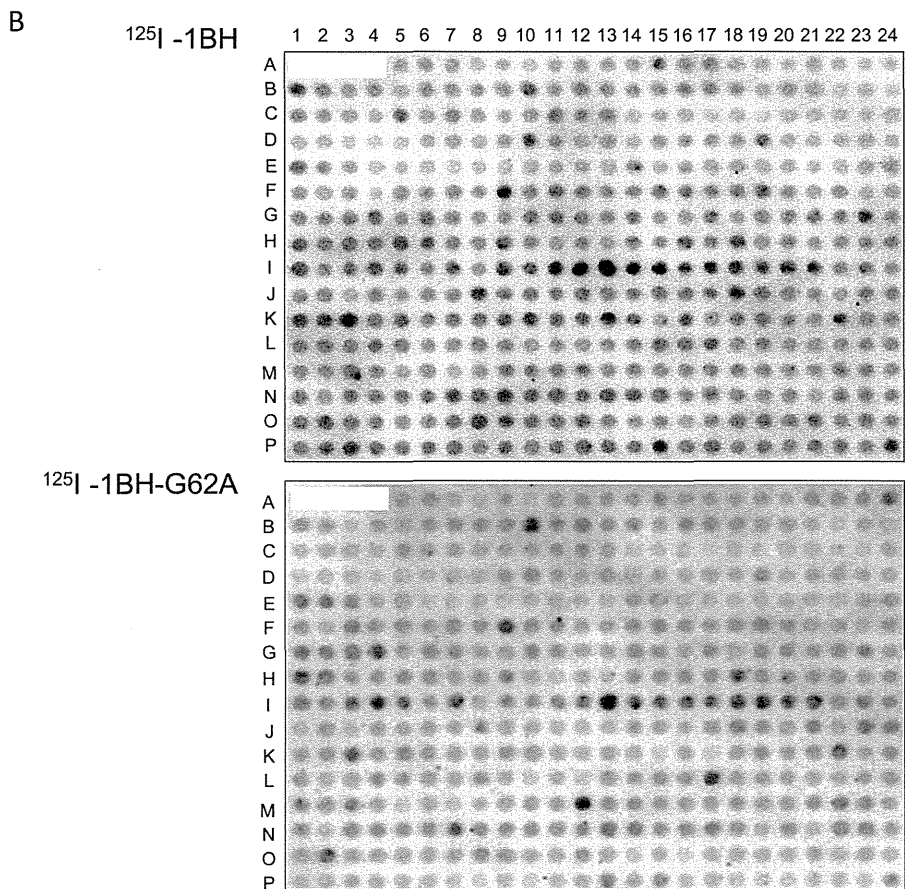
FIG 3 Screening of divalent peptides synthesized on a membrane based on binding to 1BH but not to 1BH-G62A. (A) The structure of the divalent peptide synthesized on a membrane was the same as that shown in Fig. 2A. The density of the peptides (y) was 100%, and the spacer length (n) was 1. The first three amino acids present in the XXA-RRRR or AAX-RRRR motif are shown at positions A5 to P5 or positions P6 to P23, respectively. The divalent peptide with the original motif, KRR-RRRR, was synthesized at position P24. The gray boxes indicate the 64 candidate motifs that were selected after the binding analysis. (B) The membrane was blotted with ^{125}I-1BH or ^{125}I-1BH-G62A (1 μg/ml), and the radioactivity bound to each peptide spot was quantitated and analyzed as shown in Table S1 in the supplemental material.
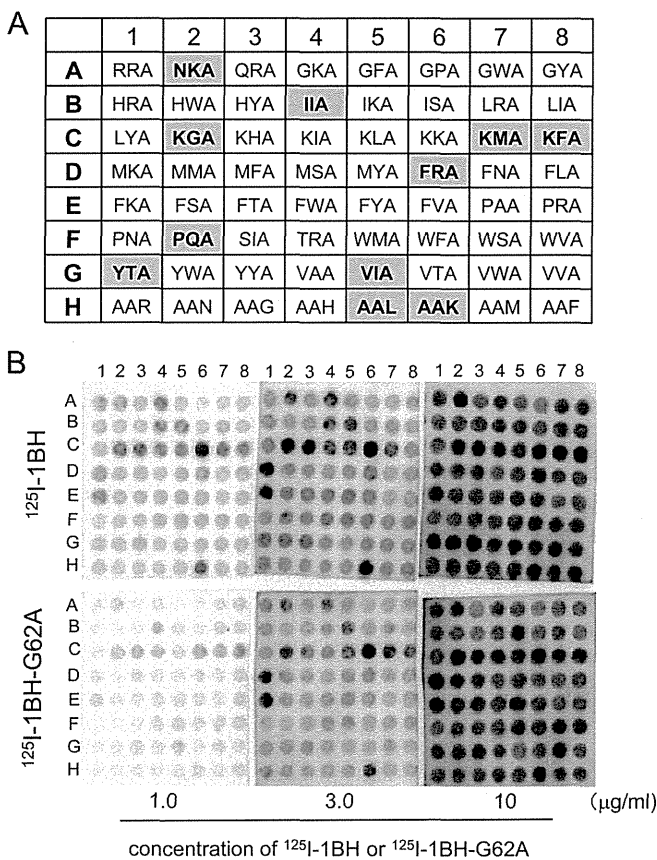
A

	1	2	3	4	5	6	7	8
A	RRA	NKA	QRA	GKA	GFA	GPA	GWA	GYA
B	HRA	HWA	HYA	IIA	IKA	ISA	LRA	LIA
C	LYA	KGA	KHA	KIA	KLA	KKA	KMA	KFA
D	MKA	MMA	MFA	MSA	MYA	FRA	FNA	FLA
E	FKA	FSA	FTA	FWA	FYA	FVA	PAA	PRA
F	PNA	PQA	SIA	TRA	WMA	WFA	WSA	WVA
G	YTA	YWA	YYA	VAA	VIA	VTA	VWA	VVA
H	AAR	AAN	AAG	AAH	AAL	AAK	AAM	AAF

B

concentration of ¹²⁵I-1BH or ¹²⁵I-1BH-G62A

FIG 4 Binding analysis of the divalent peptides with 64 candidate motifs synthesized on a membrane to 1BH or 1BH-G62A. (A) The structure of the divalent peptide synthesized on a membrane was the same as that shown in Fig. 3A. The 64 divalent peptides with candidate motifs, the first three amino acids of which are shown in the panel, were synthesized at the indicated positions. The gray boxes indicate the 11 candidate motifs selected after the binding analysis as shown in Fig. S1 in the supplemental material. (B) The membrane was blotted with the indicated amounts of ¹²⁵I-1BH or ¹²⁵I-1BH-G62A, and the radioactivity bound to each peptide spot was quantitated and analyzed (see Fig. S1 in the supplemental material).

PQA-tet, YTA-tet, VIA-tet, AAL-tet, and AAK-tet. The binding of these tetravalent peptides to 1BH or 1BH-G62A was examined (Fig. 5). All of the tetravalent peptides bound to 1BH with more potency than to 1BH-G62A, indicating that site 2 is involved in the binding of these peptides. Under the same conditions, MMA-tet, which binds to sites 1 and 3 of 1BH but not site 2 (22), bound to 1BH-G62A with similar affinity as that of 1BH (data not shown), further confirming the binding specificity of the identified tetravalent peptides. As shown in Table 1, all of these tetravalent peptides bound to 1BH with high affinities.

Tetravalent peptides with the identified motifs efficiently inhibit the cytotoxicity of Stx1a. The ability of the identified tetravalent peptides to inhibit the cytotoxicity of Stx1a in Vero cells was examined (Fig. 6). MMA-tet was used as a positive control. Among the 11 tetravalent peptides, KGA-tet, KFA-tet, FRA-tet, PQA-tet, YTA-tet, VIA-tet, and AAL-tet inhibited Stx1a cytotoxicity as efficiently as MMA-tet, although the inhibitory effects of KFA-tet and FRA-tet were reduced at 52 μM because of their own cytotoxicity (data not shown). NKA-tet, IIA-tet, KMA-tet, and AAK-tet exerted inhibitory effects with lower efficiency.

DISCUSSION

In this study, we established a novel technique to synthesize, on a single cellulose membrane, divalent peptides that could exert the clustering effect on the Stx1a B subunit. By targeting one of the receptor-binding sites (site 2) of the B subunit, we screened divalent peptides whose sequences were designed based on information obtained by multivalent peptide library screening. We successfully identified 11 peptide-based neutralizers of Stx1a. Thus, the combination of these two techniques enables us to identify a wide range of biologically active neutralizers of Stx1a, whereas the multivalent peptide library technique yielded only one motif, which was found to be cytotoxic.

Previously, we developed a series of carbosilane dendrimers with clustered trisaccharides of Gb3, named SUPER TWIGs, as Stx neutralizers (27, 30). One of these compounds, SUPER TWIG (1)2, which has a divalent form of the trisaccharide, was found to sufficiently exert the clustering effect on the Stx B subunit to markedly increase binding affinity. Their K_D (dissociation constant) values toward the Stx1a B subunit and Stx2a B subunit were determined to be 88 and 68 μM, respectively, using the Biacore system; no binding was observed with free trisaccharide up to 1.6 mM (20, 27). These observations provide a theoretical rationale for the use of membrane-synthesized divalent (but not monomeric) peptides during screening of high-affinity binding motifs against the B subunit. Furthermore, our finding that higher density and shorter spacer length of the divalent peptide resulted in higher binding efficacy clearly demonstrates that a spatially condensed configuration of the divalent peptide enables each motif to exert the clustering effect.

Here, we focused on site 2 as a target region to develop an Stx1a neutralizer because this site has already been shown to play an essential role in the receptor binding of Stx1a (26, 31, 32). One of the Stx neutralizers with clustered trisaccharides, the STARFISH compound, containing 10 trisaccharides assembled into a single glucose core through bifurcated spacers, was found to exclusively occupy site 2 of the Stx1a B subunit, further confirming the importance of site 2 as a target region (33). The 11 Stx1a neutralizers that we identified here are the first peptide-based neutralizers to target site 2, while PPP-tet and MMA-tet, which were identified by targeting site 3 of Stx2a and site 1 of Stx1a, respectively, did not touch site 2 on each B subunit (Fig. 5) (20, 22). Among these inhibitors, KGA-tet, PQA-tet, YTA-tet, VIA-tet, and AAL-tet inhibited the cytotoxicity of Stx1a with potency similar to that of MMA-tet (Fig. 6).

All the divalent peptides synthesized on a membrane have the RRRR motif at positions 4 to 7: this motif was introduced based on information obtained from multivalent peptide library screening. The addition of even a single acidic amino acid (Asp or Glu) to this motif at position 1, 2, or 3 markedly reduced the binding of ¹²⁵I-1BH and ¹²⁵I-1BH-G62A (positions C14 to D8, E4 to E22, F23, G16, G18, H11, H13, I6, I8, J1, J3, K15, K17, M5, M7, N2, and N21, in Fig. 3B), and surprisingly, no acidic amino acids were selected in the data shown in Table S1 in the supplemental material. This significant finding about the negative selectivity of acidic amino acids cannot be theoretically obtained by using the multivalent peptide library technique. In accordance with this observation, all the motifs with 1BH-binding values and 1BH-G62A values greater than 2.2 have at least one Lys in positions 1 to 3 (see Table S1 in the supplemental material), demonstrating that the
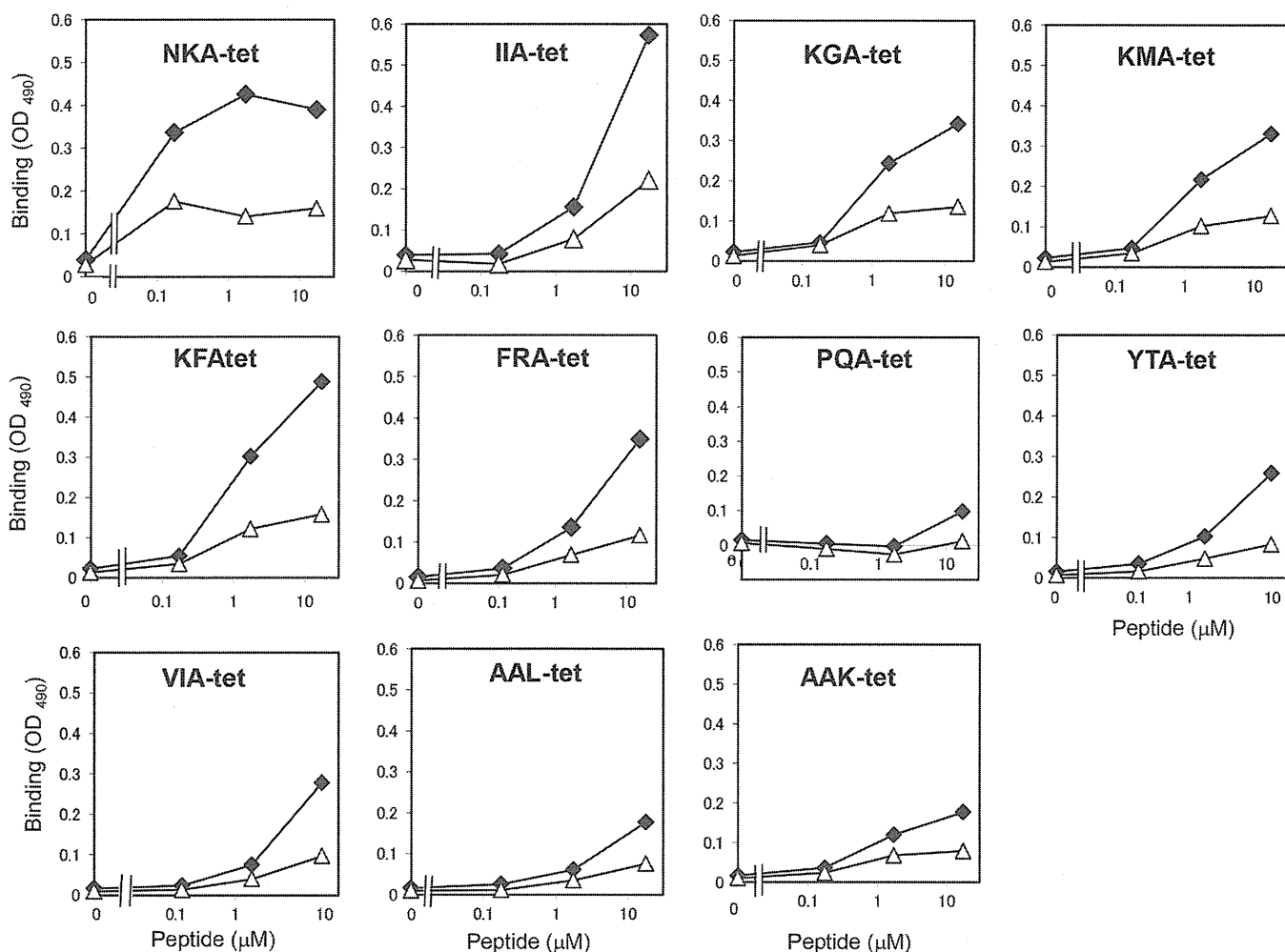
— 64 —

FIG 5 Analysis of the binding of the identified tetravalent peptides with 1BH or 1BH-G62A. The binding of 1BH (closed diamonds) or 1BH-G62A (open triangles) (1 μg/ml) with the indicated amounts of the tetravalent peptides was examined using ELISA.

basic amino acid cluster is required to efficiently bind to the B subunit, irrespective of the presence of Gly 62. It is possible that this basic amino acid cluster interacts with the acidic amino acids present on the receptor-binding surface of the B subunit (Asps 16,

TABLE 1 Binding kinetics of the identified tetravalent peptides[a]

Tetravalent peptide	K_D (μM), mean ± SE ($n = 3$)	RU_{max} (AU), mean ± SE ($n = 3$ to 4)
NKA-tet	0.28 ± 0.01	2,460 ± 57
IIA-tet	0.51 ± 0.05	3,580 ± 52
KGA-tet	0.21 ± 0.01	1,390 ± 77
KMA-tet	0.43 ± 0.03	2,510 ± 71
KFA-tet	0.55 ± 0.04	3,630 ± 44
FRA-tet	0.63 ± 0.11	3,910 ± 95
PQA-tet	0.57 ± 0.01	2,140 ± 19
YTA-tet	0.34 ± 0.03	2,170 ± 364
VIA-tet	0.40 ± 0.01	2,050 ± 202
AAL-tet	1.00 ± 0.14	2,400 ± 175
AAK-tet	0.35 ± 0.02	2,630 ± 35

[a] The binding kinetics of the identified tetravalent peptides to immobilized 1BH were analyzed using the Biacore system. K_D, dissociation constant; RU_{max}, maximum resonance unit.

17, and 18) (18) through electrostatic interactions. Thus, amino acids in other positions may contribute to binding site specificity. Specifically, 8 out of 11 identified Stx neutralizers have at least one hydrophobic amino acid in positions 1 to 3 (e.g., Ile, Met, Phe, Val, Pro, Tyr, or Leu) which might be involved in hydrophobic interactions at site 2, where hydrophobic interactions with the trisaccharide are prominent during receptor recognition compared to the other receptor-binding sites (18).

The novel membrane-screening technique established here substantially overcomes the problems of the multivalent peptide library technique, where only a limited number of binding motifs are determined and redundancy of amino acid selectivity may be observed in some positions in the motif. In this technique, hundreds of divalent peptides synthesized on a membrane with known sequences can be screened quantitatively, thus yielding a wide variety of binding motifs that could successfully distinguish a small change in amino acid sequence, such as Gly to Ala. Various closely related subtypes for Stx1 (Stx1a, -1c, and -1d) and Stx2 (Stx2a, -2b, -2c, -2d, -2e, -2f, and -2g) are present (12–14), but their modes of globosugar recognition are shown to be substantially different because of the minute differences present on the receptor-binding surface of the B subunits (34). Thus, the combi-
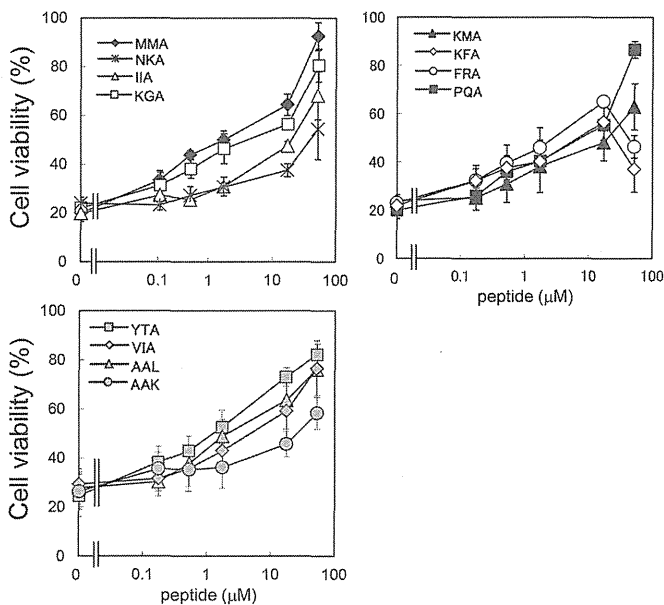
FIG 6 Inhibitory effects of the identified tetravalent peptides on the cytotoxicity of Stx1a in Vero cells. The effects of the identified tetravalent peptides on the cytotoxicity of Stx1a (1 pg/ml) in Vero cells were examined by the cytotoxicity assay. Data are presented as a percentage of the control value (mean ± standard error, $n = 3$).

nation of the two techniques presented here will provide a powerful strategy to develop optimal neutralizers against specific subtypes, enabling customized therapy that targets individual Stx subtypes produced by various EHEC strains.

ACKNOWLEDGMENTS

REFERENCES

1. Karmali MA, Steele BT, Petric M, Lim C. 1983. Sporadic cases of haemolytic uraemic syndrome associated with fecal cytotoxin and cytotoxin-producing Escherichia coli in stools. Lancet i:619–620.
2. Riley LW, Remis RS, Helgerson SD, McGee HB, Wells JG, Davis BR, Hebert RJ, Olcott ES, Johnson LM, Hargrett NT, Blake PA, Cohen ML. 1983. Hemorrhagic colitis associated with a rare Escherichia coli serotype. N Engl J Med 308:681–685. http://dx.doi.org/10.1056/NEJM198303243081203.
3. O'Brien AD, Holmes RK. 1987. Shiga and Shiga-like toxins. Microbiol Rev 51:206–220.
4. Paton JC, Paton AW. 1998. Pathogenesis and diagnosis of Shiga toxin-producing Escherichia coli infections. Clin Microbiol Rev 11:450–479.
5. Tarr PI, Gordon CA, Chandler WL. 2005. Shiga-toxin-producing Escherichia coli and haemolytic uraemic syndrome. Lancet 365:1073–1086. http://dx.doi.org/10.1016/S0140-6736(05)71144-2.
6. Trachtman H, Austin C, Lewinski M, Stahl RA. 2012. Renal and neurological involvement in typical Shiga toxin-associated HUS. Nat Rev Nephrol 8:658–669. http://dx.doi.org/10.1038/nrneph.2012.196.
7. Frank C, Werber D, Cramer JP, Askar M, Faber M, an der Heiden M, Bernard H, Fruth A, Prager R, Spode A, Wadl M, Zoufaly A, Jordan S, Kemper MJ, Follin P, Müller L, King LA, Rosner B, Buchholz U, Stark K, Krause G, HUS Investigation Team. 2011. Epidemic profile of Shiga-toxin-producing Escherichia coli O104:H4 outbreak in Germany. N Engl J Med 365:1771–1780. http://dx.doi.org/10.1056/NEJMoa1106483.
8. Hauswaldt S, Nitschke M, Sayk F, Solbach W, Knobloch JK. 2013. Lessons learned from outbreaks of Shiga toxin producing Escherichia coli. Curr Infect Dis Rep 15:4–9. http://dx.doi.org/10.1007/s11908-012-0302-4.
9. Ikeda K, Ida O, Kimoto K, Takatorige T, Nakanishi N, Tatara K. 1999. Effect of early fosfomycin treatment on prevention of hemolytic uremic syndrome accompanying Escherichia coli O157:H7 infection. Clin Nephrol 52:357–362.
10. Wong CS, Jelacic S, Habeeb RL, Watkins SL, Tarr PI. 2000. The risk of the hemolytic-uremic syndrome after antibiotic treatment of Escherichia coli O157:H7 infections. N Engl J Med 342:1930–1936. http://dx.doi.org/10.1056/NEJM200006293422601.
11. Wong CS, Mooney JC, Brandt JR, Staples AO, Jelacic S, Boster DR, Watkins SL, Tarr PI. 2012. Risk factors for the hemolytic uremic syndrome in children infected with Escherichia coli O157:H7: a multivariable analysis. Clin Infect Dis 55:33–41. http://dx.doi.org/10.1093/cid/cis299.
12. Gyles CL. 2007. Shiga toxin-producing Escherichia coli: an overview. J Anim Sci 85:E45–E62. http://dx.doi.org/10.2527/jas.2006-508.
13. Fuller CA, Pellino CA, Flagler MJ, Strasser JE, Weiss AA. 2011. Shiga toxin subtypes display dramatic differences in potency. Infect Immun 79:1329–1337. http://dx.doi.org/10.1128/IAI.01182-10.
14. Scheutz F, Teel LD, Beutin L, Piérard D, Buvens G, Karch H, Mellmann A, Caprioli A, Tozzoli R, Morabito S, Strockbine NA, Melton-Celsa AR, Sanchez M, Persson S, O'Brien AD. 2012. Multicenter evaluation of a sequence-based protocol for subtyping Shiga toxins and standardizing Stx nomenclature. J Clin Microbiol 50:2951–2963. http://dx.doi.org/10.1128/JCM.00860-12.
15. Karmali MA, Petric M, Lim C, Fleming PC, Arbus GS, Lior H. 1985. The association between idiopathic hemolytic uremic syndrome and infection by verotoxin-producing Escherichia coli. J Infect Dis 151:775–782. http://dx.doi.org/10.1093/infdis/151.5.775.
16. Melton-Celsa AR, O'Brien AD. 1998. Structure, biology, and relative toxicity of Shiga toxin family members for cells and animals, p 121–128. In Kaper JB, O'Brien AD (ed), Escherichia coli O157:H7 and other Shiga toxin-producing E. coli strains. ASM Press, Washington, DC.
17. DeGrandis S, Law H, Brunton J, Gyles C, Lingwood CA. 1989. Globotetraosylceramide is recognized by the pig edema disease toxin. J Biol Chem 264:12520–12525.
18. Ling H, Boodhoo A, Hazes B, Cummings MD, Armstrong GD, Brunton JL, Read RJ. 1998. Structure of the Shiga-like toxin I B-pentamer complexed with an analogue of its receptor Gb3. Biochemistry 37:1777–1788. http://dx.doi.org/10.1021/bi971806n.
19. Fraser ME, Fujinaga M, Cherney MM, Melton-Celsa AR, Twiddy EM, O'Brien AD, James MNG. 2004. Structure of Shiga toxin type 2 (Stx2) from Escherichia coli O157:H7. J Biol Chem 279:27511–27517. http://dx.doi.org/10.1074/jbc.M401939200.
20. Nishikawa K, Watanabe M, Kita E, Igai K, Omata K, Yaffe MB, Natori Y. 2006. A multivalent peptide library approach identifies a novel Shiga toxin inhibitor that induces aberrant cellular transport of the toxin. FASEB J 20:2597–2599. http://dx.doi.org/10.1096/fj.06-6572fje.
21. Watanabe-Takahashi M, Sato T, Dohi T, Noguchi N, Kano F, Murata M, Hamabata T, Natori Y, Nishikawa K. 2010. An orally applicable Shiga toxin neutralizer functions in the intestine to inhibit the intracellular transport of the toxin. Infect Immun 78:177–183. http://dx.doi.org/10.1128/IAI.01022-09.
22. Tsutsuki K, Watanabe-Takahashi M, Takenaka Y, Kita E, Nishikawa K. 2013. Identification of a peptide-based neutralizer that potently inhibits both Shiga toxins 1 and 2 by targeting specific receptor-binding regions. Infect Immun 81:2133–2128. http://dx.doi.org/10.1128/IAI.01256-12.
23. Ostroff SM, Tarr PI, Neill MA, Lewis JH, Hargrett-Bean N, Kobayashi JM. 1989. Toxin genotypes and plasmid profiles as determinants of systemic sequelae in Escherichia coli O157:H7 infections. J Infect Dis 160:994–998. http://dx.doi.org/10.1093/infdis/160.6.994.
24. Tesh VL, Burris JA, Owens JW, Gordon VM, Wadolkowski EA, O'Brien AD, Samuel JE. 1993. Comparison of the relative toxicities of Shiga-like toxins type I and type II for mice. Infect Immun 61:3392–3402.
25. Stearns-Kurosawa DJ, Collins V, Freeman S, Debord D, Nishikawa K, Oh SY, Leibowitz CS, Kurosawa S. 2011. Rescue from lethal Shiga toxin 2-induced renal failure with a cell-permeable peptide. Pediatr Nephrol 26:2031–2039. http://dx.doi.org/10.1007/s00467-011-1913-y.

26. Soltyk AM, MacKenzie CR, Wolski VM, Hirama T, Kitov PI, Bundle DR, Brunton JL. 2002. A mutational analysis of the globotriaosylceramide-binding sites of verotoxin VT. J Biol Chem 277:5351–5359. http://dx.doi.org/10.1074/jbc.M107472200.

27. Nishikawa K, Matsuoka K, Watanabe M, Igai K, Hino K, Terunuma D, Kuzuhara H, Natori Y. 2005. Identification of the optimal structure for a Shiga toxin neutralizer with oriented carbohydrates to function in the circulation. J Infect Dis 191:2097–2105. http://dx.doi.org/10.1086/430388.

28. Frank R. 1992. Spot-synthesis: an easy technique for the positionally addressable, parallel chemical synthesis on a membrane support. Tetrahedron 48:9217–9232. http://dx.doi.org/10.1016/S0040-4020(01)85612-X.

29. Frank R. 2002. The SPOT-synthesis technique. Synthetic peptide arrays on membrane supports—principles and applications. J Immunol Methods 267:13–26. http://dx.doi.org/10.1016/S0022-1759(02)00137-0.

30. Nishikawa K, Matsuoka K, Kita E, Okabe N, Mizuguchi M, Hino K, Miyazawa S, Yamasaki C, Aoki J, Takashima S, Yamakawa Y, Nishijima M, Terunuma D, Kuzuhara H, Natori Y. 2002. A therapeutic agent with oriented carbohydrates for treatment of infections by Shiga toxin-producing Escherichia coli O157:H7. Proc Natl Acad Sci U S A 99:7669–7674. http://dx.doi.org/10.1073/pnas.112058999.

31. Wolski VM, Soltyk AM, Brunton JL. 2001. Mouse toxicity and cytokine release by verotoxin 1B subunit mutants. Infect Immun 69:579–583. http://dx.doi.org/10.1128/IAI.69.1.579-583.2001.

32. Flagler MJ, Mahajan SS, Kulkarni AA, Iyer SS, Weiss AA. 2010. Comparison of binding platforms yields insights into receptor binding differences between Shiga toxins 1 and 2. Biochemistry 49:1649–1657. http://dx.doi.org/10.1021/bi902084y.

33. Kitov PI, Sadowska JM, Mulvey G, Armstrong GD, Ling H, Pannu NS, Read RJ, Bundle DR. 2000. Shiga-like toxins are neutralized by tailored multivalent carbohydrate ligands. Nature 403:669–672. http://dx.doi.org/10.1038/35001095.

34. Yosief HO, Iyerb SS, Weiss AA. 2013. Binding of Pk-trisaccharide analogs of globotriaosylceramide to Shiga toxin variants. Infect Immun 81:2753–2760. http://dx.doi.org/10.1128/IAI.00274-13.

厚生労働科学研究委託費（創薬基盤推進研究事業）

医薬品・医療機器の実用化促進のための評価技術手法の戦略的開発
（H26-創薬-一般-008）

平成26年度　委託業務成果報告書
第6/7分冊　研究分担報告書

テーマ2-3　新規培養基材等を用いた肝代謝・
動態等評価系の開発

担当責任者：石田 誠一　国立医薬品食品衛生研究所 薬理部
担当責任者：青山 晋輔　積水メディカル株式会社
担当責任者：竹澤 俊明　独立行政法人農業生物資源研究所
担当責任者：柿木 基治　エーザイ株式会社
担当責任者：立野（向谷）知世　株式会社フェニックスバイオ
担当責任者：最上 知子　国立医薬品食品衛生研究所 代謝生化学部
担当責任者：田辺 宗平　興和株式会社

目　　次

厚生労働科学研究委託費（創薬基盤推進研究事業）
委 託 業 務 成 果 究 報 告 書（業 務 項 目）

担 当 研 究 課 題　　テーマ総括、新規肝代謝・動態等評価法の開発
　　　　　　　　　及びヒト肝細胞等の機能評価と安全性評価法への応用の検討

担当責任者　石田誠一　国立医薬品食品衛生研究所　薬理部室長
担当責任者　青山晋輔　積水メディカル株式会社　主任研究員

研究要旨
　コラーゲンプレートで PXB 細胞を培養したところ、HepaRG の 1/4 程度の CYP3A4 の酵素活性と omeprazole による約 19 倍の CYP1A2 の発現誘導が観察された。HpaRG 細胞と PXB 細胞の代謝活性が向上することを期待して ad-MED ビトリゲル®で培養したところ、いずれの細胞も良好な接着性を示した。Ad-MED ビトリゲル®培養により、HepaRG における CYP1A2 の発現の上昇が観察された。しかし、CYP3A4 による代謝（LC-MS/MS、real-time PCR）に関しては、どちらの細胞においても変化が観察できなかった。HepG2 による化合物の毒性試験では、細胞への毒性が予想される化合物において濃度依存的な生存活性の低下が観察され、PXB 細胞や HepaRG 細胞を用いて毒性試験を行う際の基礎データを得ることができた。

研究協力者
堀内新一郎　国立医薬品食品衛生研究所
　　　　　　非常勤職員

A. 研究目的
　新規薬物の開発段階において、薬効及び安全性を評価するために候補化合物の代謝経路とそれに及ぼす影響を精査することは必須である。多くの外来物質の代謝を担う中心的な臓器は肝臓であり、その機能を担うヒト肝実質細胞がこの目的のために多用されている。しかしながら、その入手は一部を除き海外に依存しており、安定しておらず、個人差に由来するばらつきも存在する。したがって、細胞機能の再現性や倫理性の観点から、新規薬物候補化合物の評価系として必ずしも適切なものとはなっていない。そこで本研究では、安定な実験が可能で、よりヒト肝臓の代謝機能を模倣している系を確立することを目的と

している。
　本研究には HepaRG 細胞と PXB 細胞を用いた。HepaRG 細胞はフランス INSERM において C 型肝炎患者から樹立された肝実質細胞前駆培養細胞株であり、肝実質細胞様に分化すること、および、分化状態では肝実質細胞とほぼ同等の細胞機能を示すことが明らかにされている。また、PXB 細胞は、（株）フェニックスバイオ社のヒトキメラマウス由来の hepatocyte で、このマウスはヒトの肝細胞の移植によって、肝臓の 70%〜90% 以上が正常ヒト肝細胞に置換されている。このため PXB マウスの肝臓では、ヒトアルブミンの産生、ヒト代謝酵素及びトランスポーターの発現および活性、ヒト型の胆汁酸組成などが確認されている。
　ad-MED ビトリゲル®上で HepG2 を培養すると通常のプレートで培養した場合と比較して代謝活性（3A4）が高くなることを確認し

ている。ビトリゲルとは、コラーゲンハイドロゲルを低温、低湿下でガラス化したもので、これを培養基に応用し商品化したのもがad-MED ビトリゲル®である。

本研究では PXB 細胞の代謝、誘導試験への応用を目指し、PXB 細胞の薬物代謝、及び誘導能を評価した。更に ad-MED ビトリゲル®を用いることにより HpaRG 細胞と PXB 細胞の代謝活性が向上することを期待し、両細胞を ad-MED ビトリゲル®で培養した。また、PXB 細胞や HepaRG で化合物の毒性試験を行う際の基礎データを得るために、HepG2 細胞で様々な化合物に対する毒性試験を行った。

B. 研究方法
HepaRG 細胞の培養と分化誘導

HepaRG 細胞の培養は、Williams' medium E (invitrogen 社) 培地に 10% FBS、2 mM glutamine、5 μg/mL insulin、50 μM hydrocortisone、50 U/mL penicillin and streptomycin を加えたものを用いて、5% CO_2 を含む気相下 37℃で行った。肝実質細胞への分化誘導は、播種後 14 日目から 28 日目まで培地中に2% DMSO を添加することにより行った。

分化した肝実質細胞を培養する際には、分化を維持するために、細胞回収前の2倍の細胞密度で細胞を播種し培養を行った。また、細胞を小さな塊の状態で播種するために、トリプシン処理後、必要以上にピペッティングせずに細胞の塊が残った状態にした。

PXB 細胞の培養

PXB 細胞は、（株）フェニックスバイオ社にて Ad-MED ビトリゲル®とコラーゲンコートプレートに細胞を播種し、2 日間培養した後、陸路にて国立医薬品食品衛生研究所まで輸送した。細胞の培養は、5% CO_2 を含む気相下 37℃で行った。培養には dHCGM 培地（フェノールレッド不含）を用いた。

PXB 細胞における薬物代謝誘導試験

コラーゲンコートプレートで培養中の PXB 細胞に 25μM omeprazole（in DMSO）を 1/500 量（終濃度 50nM）添加して 1 日間培養し、RNA を回収した。また、比較のために 0.2%DMSO を添加した条件で 1 日間培養を行った。

ビトリゲル®培養

Ad-MED ビトリゲル®（関東化学）を再水和するために、下層部分（12 ウェルプレート）に 1.5ml の PBS を加え、更に ad-MED ビトリゲル®インサート（上層部）に 0.3ml の PBS を加え、ゲル部分が透明になるまで室温で静置した。再水和終了後、下層とインサートの PBS を取り除き、下層部へ培養に用いる培地を 1.5ml 加え、インサートを設置した。それぞれの細胞の懸濁液を用意し、所定の細胞密度（PXB：2.1×10⁵ cells/cm²、HepaRG：播種前の 2 倍の細胞密度）になるようにインサートに播種した。培養期間中の培養液量は下層 1.5ml、インサート 0.3ml とした。また、Ad-MED ビトリゲル®培養では、下層に培養液を入れた状態での培養を液相-液相培養、下層に培養液を入れず、気相にした状態での培養を液相-気相培養とした。

コラーゲンコートプレートによる培養

Ad-MED ビトリゲル®培養と細胞の接着や形状、代謝活性を比較するために、それぞれの細胞をコラーゲンでコートされたプレートで培養した。それぞれの細胞懸濁液を用意し、所定の細胞密度（PXB：2.1×10⁵ cells/cm²、HepRG：播種前の 2 倍の細胞密度）となるように播種した。培養期間中の培養液量は 0.225ml とした。

LC-MS/MS による代謝活性測定

1mM の midazoram 溶液（in DMSO）を作成し、それぞれの培地に 1/1000 量添加して midazoram 添加培地とした。Ad-MED ビトリゲル®培養、コラーゲンプレート培養の培養液を midazoram 添加培地に置き換えた。この際、培地の量は ad-MED ビトリゲル®培養が 0.280ml、コラーゲンプレート培養は 0.218ml とした。midazoram 添加培地で培養はじめた後、0、1、2 時間目に 30µl の培養液を回収して LC-MS/MS のサンプルとした。サンプルは直ちに-80℃で保存し、後日、ドライアイス梱包にて積水メディカル株式会社に発送した。積水メディカルでは、midazoram の代謝産物である 1'-OH midazolam を LC-MS/MS にて測定した。LC-MS/MS 分析には、測定サンプル（30 µL）にアセトニトリル（10 µL）又は内標準溶液（10 µL）を混合し，遠心分離（条件：10,000×g，4℃，5分）にて除蛋白した上清を用いた。LC-MS/MS 分析の詳細な条件は表.1 に示した。

P450-Glo による代謝活性

CYP3A4 の酵素活性を P450-Glo CYP3A4 Assay (Luciferin-IPA)を用いて測定した。測定は添付の資料に従って行った。P450-Glo の測定結果は CellTiter-Glo によって測定した生存活性で割ることによって規格化を行った。

real-time PCR

PXB 細胞と HepaRG 細胞からの RNA の抽出は、RNeasy mini kit (QIAGEN 社)を用いて行った。調製した total RNA は、各サンプルにつき HepaRG 細胞は 200ng、PXB 細胞は 150ng を TaqMan Reverse Transcription Reagent (Applied Biosystems 社)を用い、添付の方法に従い、Oligo dT(16) をプライマーとして逆転写した。逆転写産物は、TaqMan Universal PCR Master Mix (Applied Biosystems 社)と各種遺伝子に特異的な TaqMan プライマー (Applied Biosystems 社)を用いて ViiA™7 real time PCR system (Applied Biosystems 社)により発現量を測定した。

HepG2 による化合物の毒性試験

HepG2 細胞を 96 ウェルプレートに 4.24×10⁴ cells 播種した。24 時間後、培養液を化合物添加培地に置換して化合物への曝露を開始した。化合物曝露 24 時間目に化合物添加培地の交換を行い、曝露開始 48 時間目に CellTiter-Glo により生存活性を評価した。毒物試験には以下の化合物を使用した。アセトアミノフェン、塩化銅、アミオダロン塩酸塩、シクロホスファミド水和物、フルタミド メフェナム酸、ノボビオシン、シプロヘプタジン、チクロビジン。また、ネガティブコントロールには、アスピリン、フルオキセチン、メラトニン、ロシグリタゾンを用いた。

（倫理面への配慮）
本年度は該当事項なし

C. 研究結果
1) コラーゲンコートプレートによる PXB 細胞の培養

コラーゲンコートプレートにおいて PXB 細胞を 8 日間培養した（図 1）。
細胞の様子

8 日目において、プレートに接着した細胞の形状は、肝実質細胞様の形状（敷石状）をしており、ウェル間に差がなかった（図 2）。
P450-Glo による代謝酵素活性の測定

6 日間培養した HepaRG 細胞と CYP3A4 活性を比較したところ、PXB 細胞の CYP3A4 活性は HepaRG 細胞の約 1/4 であった（図 3）。この際、PXB 細胞において、CellTiter-Glo による生存活性が同じにもかかわらず、CYP3A4 活性がウェル間で差が生じた。一方、

HepaRG 細胞の CYP3A4 活性はウェル間で差がなかった。

real-time PCR による代謝誘導試験

　omeprazole に 1 日間暴露し、CYP3A4 と CYP1A2 の発現を real-time PCR により測定した。RNA の回収量が少なかったため、Control は n=2、0.2%DMSO と omeprazole 添加が、それぞれ n=1 の結果である。omeprazole により CYP1A2 の発現が 19.5 倍誘導された（図 4）。

2) Ad-MED ビトリゲル®による HepaRG 細胞の培養

　Ad-MED ビトリゲル®における培養では、HepaRG 細胞を十分に接着させるために 4 日間の液相-液相培養を行い、その後、液相-液相培養を続けるものと液相-気相培養へ移行するものへと分けた（図 5）。

細胞の様子

　ad-MED ビトリゲル®への細胞播種から液相-液相培養と液相-気相培養に分ける直前までにおいて、細胞の接着、形状はコラーゲンコートプレートでの培養と比較して顕著な違いは観察できなかった。液相-気相と液相-液相に分けた後においても、ad-MED ビトリゲル®上に接着している細胞の形状に変化はなかった（図 6）。

LC-MS/MS による代謝活性測定

　LC-MS/MS を用いて midazolam の代謝産物である 1'-OH midazolam を測定（n=3）し、CYP3A4 の代謝活性を評価した。液相-液相培養ではインサート部分の培養液が下層に拡散してしまうため、インサート部分の培養液と下層部分の培養液が平衡化しているものと仮定して、液相-液相の測定値を 7 倍に換算し評価した。

　HepaRG では、気相培養の代謝活性がコラーゲンコートプレートの培養より低くなっていた（図 7）。

real-time PCR による CYP450 の発現測定

　real-time PCR により CYP3A4 と 1A2 の発現を測定（n=3）した。CYP1A2 の発現が液相-液相培養で最も高く、液相-気相培養でもコラーゲンコートプレートでの培養より高くなっていた（図 7）。CYP3A4 の発現はコラーゲンコートプレートでの培養で最も高かった。

3) Ad-MED ビトリゲル®による PXB 細胞の培養

　Ad-MED ビトリゲル®における培養では、PXB 細胞を十分に接着させるために 6 日間の液相-液相培養を行い、その後、液相-液相培養を続けるものと液相-気相培養へ移行するものへと分けた（図 1）。

細胞の様子

　ad-MED ビトリゲル®への細胞播種から液相-液相培養と液相-気相培養に分ける直前までにおいて、細胞の接着、形状はコラーゲンコートプレートでの培養と比較して顕著な違いは観察できなかった。液相-気相と液相-液相に分けた後においても、ad-MED ビトリゲル®上に接着している細胞の形状に変化はなかった（図 8）。しかし、液相-気相培養において（ad-MED ビトリゲル®上ではなく）細胞上に重層していた細胞が、液相-液相培養と比較して、より多く剥がれていた。

LC-MS/MS による代謝活性測定

　LC-MS/MS を用いて midazolam の代謝産物である 1'-OH midazolam を測定（n=3）し、CYP3A4 の代謝活性を評価した。液相-液相培養ではインサート部分の培養液が下層に拡散してしまうため、インサート部分の培養液と下層部分の培養液が平衡化しているものと仮定して、液相-液相の測定値を 7 倍に換算し評価した。

　液相-液相培養、液相-気相培養の代謝活性が共にコラーゲンコートプレートより若干高くなる傾向が観察されたが、ウェル間における差が大きく、有意な差はなかった（図 9）。

real-time PCR による CYP450 の発現測定

　real-time PCR により CYP3A4 と 1A2 の発現を測定（n=3）した。CYP3A4 と 1A2 の発現は、いずれもコラーゲンコートプレートでの培養で最も高くなっていた（図9）。

4）HepG2 による化合物の毒性試験

　フルタミドやアミオダロン塩酸塩を添加した際の HepG2 の生存活性を図10に示した。いずれも濃度依存的に生存活性が低下した。その他の化合物（アセトアミノフェン、塩化銅、アミオダロン塩酸塩、シクロホスファミド水和物、フルタミド　メフェナム酸、ノボビオシン、シプロヘプタジン、チクロビジン）を用いた場合にも濃度依存的に生存活性が低下した。なお、ネガティブコントロールとなる化合物（アスピリン、フルオキセチン、メラトニン、ロシグリタゾン）では、生存活性の低下は観察できなかった。

D．考察
1）コラーゲンコートプレートによる PXB 細胞と HepaRG 細胞の培養

　LC-MS/MS における代謝産物の測定では、PXB 細胞における Basal の CYP3A4 活性が、HepeRG と同程度であった。また、PXB 細胞における P450-Glo による CYP3A4 活性とリアルタイム PCR による CYP3A4 の発現は、HepaRG より低い値であったが、同じオーダーの値であった。更に PXB 細胞における Omeprazole による誘導実験では、19.5 倍の CYP1A2 の発現誘導が確認された。以上のことより、PXB 細胞は代謝試験、誘導試験のいずれにおいてもヒト肝実質細胞の代替細胞になりうる可能性があると考えられる。なお、今回、全ての測定事項において、PXB 細胞は HepaRG と比較して測定値のばらつきが大きくなった。この原因を解明するために、再度実験が必要であると考えられる。

2）Ad-MED ビトリゲル®による PXB 細胞と HepaRG 細胞の培養

　HepaRG を ad-MED ビトリゲル®で培養した場合、CYP3A4 に関しては、代謝活性、遺伝子発現のいずれにおいてもコラーゲンコートプレートより高くなることはなかった。HepRG における CYP1A2 の発現に関しては、コラーゲンコートプレートの培養より ad-MED ビトリゲル®おける液相-気相培養、液相-液相培養の方が高くなった。また、PBX 細胞に関しては、CYP3A4 の代謝酵素活性や発現、CYP1A2 の発現が、コラーゲンコートプレートでの培養より ad-MED ビトリゲル®での培養で有意に高くなることはなかった。以上のことより、ad-MED ビトリゲル®を培養に用いることで薬物代謝活性を全体的に向上させることは難しいが、一部の代謝酵素の活性や発現を向上させることは期待できる。このため代謝酵素の発現を一括して調べることにより、ad-MED ビトリゲル®によって向上する代謝酵素を新たに見つけることができるかもしれない。

3）HepG2 による化合物の毒性試験

　HepG2 が様々な化合物に反応し、化合物の濃度依存的に生存活性が低下した。この結果より、PXB 細胞や HepaRG 細胞を用いた毒性試験の際の化合物の濃度を決定するための指針となる各化合物の毒性に関する基礎データを得ることができた。

E．結論

　PXB 細胞が HepaRG 細胞と遜色のない代謝活性、薬物代謝誘導能を有していることを明らかにした。このことより、ヒト肝実質細胞の代替細胞として、PXB 細胞を薬物代謝や薬物代謝誘導試験へ応用できる可能性が示された。しかし、PXB 細胞では、HepaRG と比較してウェル間における薬物代謝活性の差が大きく、このため、再度、PXB 細胞におい

て実験を行い、この差が実験の手技によるものなのか、細胞に由来するものなのかを明らかにする必要がある。また、細胞に由来すものであった場合、培養方法を含め、安定した結果が得られる条件を検討する必要がある。

ad-MED ビトリゲル®が HepaRG の CYP1A2 の発現を亢進することを明らかにした。しかし、その他の項目では ad-MED ビトリゲル®が代謝活性を上げる結果は得られず、ad-MED ビトリゲル®によって薬物代謝全体を向上させるためには、更なる培養条件の検討が必要である。また、薬物代謝酵素の発現を一括して調べることができる方法、例えば三菱レーヨンのジェノパールなどを用いることにより、ad-MED ビトリゲル®により発現が亢進する新たな薬物代謝酵素を見つけることができるかもしれない。

HepG2 による化合物の毒性試験では、細胞への毒性が予想される化合物において濃度依存的な生存活性の低下が観察され、PXB 細胞や HepaRG 細胞を用いて毒性試験を行う際の基礎データを得ることができた。

F. 健康危機情報
　該当なし

G. 研究発表等

論文発表等
1) Dubois-Pot-Schneider H, Fekir K, Coulouarn C, Glaise D, Aninat C, Jarnouen K, Le Guével R, Kubo T, Ishida S, Morel F, Corlu A.: Inflammatory cytokines promote the retrodifferentiation of tumor-derived hepatocyte-like cells to progenitor cells. *Hepatology*, 2014; 60: 2077-2090.

学会発表等
1) 石田誠一、久保崇、北條麻紀、黒田幸恵、金秀良、関野祐子：VECELL 培養器を用いた肝星細胞培養の検討. 日本組織培養学会 第 87 回大会（2014, 5, 東京）
2) 松下琢、石井貴晃、市川雄大、金秀良、石田誠一、宮島敦子、関野祐子：胎児及び成人肝細胞のメタボロームと化学物質毒性発現の比較解析. 日本組織培養学会 第 87 回大会（2014, 5, 東京）
3) 石田誠一、金秀良、久保崇、黒田幸恵、北條麻紀、宮島敦子、松下琢、関野祐子：ヒト胎児および成人肝細胞のメタボローム解析による基礎代謝能の比較と化学物質による毒性発現の比較解析. 第 41 回日本毒性学会学術年会（2014, 7, 神戸）
4) Ishida S, Kim S, Kubo T, Kuroda Y, Ishii T, Hojyo M, Miyajima A, Matsushita T Sekino Y. : COMPARATIVE ANALYSIS OF HUMAN FETAL AND ADULT HEPATOCYTES BY METABOLOMICS AND GENOMICS. 第 29 回日本薬物動態学会・第 19 回国際薬物動態学会合同年会（2014, 10, サンフランシスコ）
5) 石田誠一、シュナイダー　ヘレナ、久保崇、堀環、堀内新一郎、黒田幸恵：ヒト肝前駆細胞 HepaRG の分化過程のゲノミクス/エピジェネティクス解析. 日本動物実験代替法学会　第 27 回大会（2014, 12, 横浜）
6) 石田誠一：肝臓の代謝酵素誘導評価法の確立. 第 11 回医薬品レギュラトリーサイエンスフォーラム　ヒト iPS 細胞を利用した安全性薬理試験法の実現に向けて（2014, 12, 東京）
7) 石田誠一、久保崇、北条麻紀、黒田幸恵、金秀良、関野裕子：新規培養基材で培養した星細胞培養細胞 LI90 の機能変化の解析. 第 28 回肝類洞壁細胞研究会学術集会（2014, 12, 岡山）